IEEE Open Journal of Nanotechnology

Received 21 October 2022; revised 15 November 2022; accepted 15 November 2022. Date of publication 23 November 2022; date of current version 22 December 2022. The review of this article was arranged by Associate Editor Attila Bonyar.

Digital Object Identifier 10.1109/OJNANO.2022.3224229

Additive Manufacturing for Nano-Feature Applications: Electrohydrodynamic Printing as a Next-Generation Enabling Technology

GORAN MISKOVIC AND ROBIN KAUFHOLD

Silicon Austria Labs, A-9524 Villach, Austria

CORRESPONDING AUTHOR: GORAN MISKOVIC (e-mail: goran.miskovic@silicon-Austria.com)

ABSTRACT Regardless of the technology, additive or subtractive, the miniaturization trend is constantly pushing for smaller resolutions. The rise of global challenges in material availability, fabrication in three dimensions (3D), design flexibility and rapid prototyping have pushed additive manufacturing (AM) into the spotlight. Addressing the miniaturization trend, AM has already successfully answered the challenges for microscale 3D fabrication. However, fabricating nano-resolution still presents a challenge. In this review, we will present some of the most reported AM-based technologies capable of nanoscale 3D fabrication addressing resolutions of $\leq$ 500 nm. The focus is placed on Electrohydrodynamic (EHD) printing (also known as e-jet printing), as EHD printing seems to have the best trade-off when it comes to technique complexity, achievable resolutions, material diversity and potential to scale-up throughput. An overview of the smallest achieved resolutions as well as the most unique use cases and demonstrated applications will be addressed in this work.

INDEX TERMS Electrohydrodynamic (EHD) printing, additive manufacturing (AM), 3D printing, sub-micrometer, nanometer resolution.

LIST OF ABBREVIATIONS

2PP	two-photon polymerization.
3D	three-dimensional.
AC	alternating current.
AM	additive manufacturing.
AFM	atomic force microscopy.
AZO	aluminum-doped zinc oxide.
DC	direct current.
DNA	deoxyribonucleic acid.
EHD	electrohydrodynamic.
FEBID	focused electron beam induced deposition.
FIBID	focused ion beam induced deposition.
fluidFM	fluidic force microscopy.
ITO	indium tin oxide.
LIFT	laser-induced forward transfer.
PEDOT:PSS	poly(3,4-ethylenedioxythiophene) polystyrene sulfonate.
PEO-PCL	poly(ethylene oxide) - poly(ε-caprolactone).
PMMA	poly(methyl methacrylate).
PVP	polyvinylpyrrolidone.
PZT	lead zirconate titanate.
RNA	ribonucleic acid.
SICM	scanning ion conductance microscope.
ZTO	zinc-tin-oxide.

I. INTRODUCTION

Additive manufacturing (AM) is often referred to as one of the key enabling technologies capable of answering major challenges of tomorrow and according to the ECS report [1], by 2025 AM market is expected to reach a value of €6.3 billion mainly based on the consumer electronics, automotive and aerospace industries. The most distributed AM technologies are for sure inkjet, aerosol printing, direct ink writing and laser-induced forward transfer (LIFT) just to name a few. The major advantages of AM are quite obvious: maskless fabrications, flexible and rapid prototyping, printing over 3D structured substrates, waste reduction and responsible material consumption. However, AM also faces disadvantages such as relatively low diversity of the printable materials, low printing speeds, low throughput (restricted printing size &

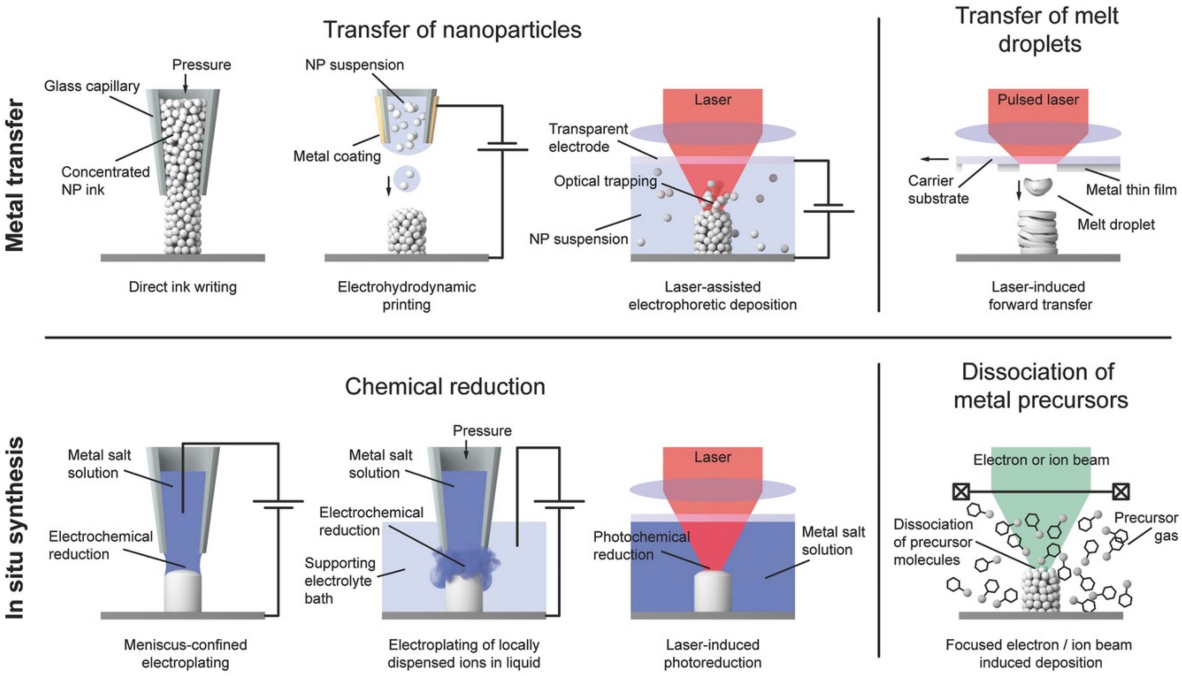

FIGURE 1. **Overview of the different technologies for additive manufacturing of high-resolution metal structures. Reproduced with permission [3] Copyright 2017, WILEY-VCH Verlag GmbH & Co. KGaA, Weinheim.**

small volumes) and relatively high electrical resistivity of the printed metal structures. Despite having all of those limitations, the advantages of AM are still deemed to be of great value for applied R&D and therefore are being intensively investigated and reported within the scientific community. The constant pursuit of Moore's law and consequently miniaturization are the main drivers for the development of novel next-generation AM technologies. The main goal put in front of them is the capability to deliver submicron resolution, with higher speeds, higher throughputs and a large portfolio of printable materials. Up to this date, the challenge of microscale fabrication has been pretty much answered and a variety of AM technologies for microscale 3D fabrication are reported [2], [3], [4], [5], [6]. In our opinion, the challenge for the AM of nanoscale fabrication will be the next goal following the miniaturization pursuit. To our best knowledge, there are no reports available addressing the AM technologies for nanoscale 3D fabrication and therefore we have taken up the challenge of providing one. There is no exact definition of where nano labeling exactly starts and where it stops, therefore for this review we took the freedom and defined 500 nm resolution to be the upper limit for nano labeling. In addition, to identify the technologies, we will also engage in a detailed analysis of the most prominent technological representatives, focusing not only on the nanoscale fabrication aspect but also on the printed materials and demonstrated applications.

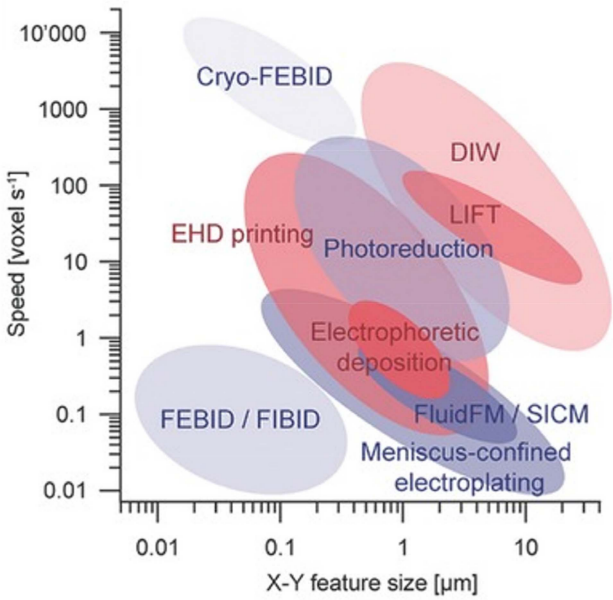

FIGURE 2. **Comparison of AM technologies with regard to their resolution and process speed. Reproduced with permission [3] Copyright 2017, WILEY-VCH Verlag GmbH & Co. KGaA, Weinheim.**

II. ADDITIVE MANUFACTURING TECHNOLOGIES FOR NANOSCALE METAL STRUCTURING

As already stated, there are several comprehensive reports addressing the AM technologies for microscale 3D fabrication [2], [3], [4], [5], [6], therefore our work will build on them. In Fig. 1., an overview of different technologies is shown, with some of them capable of achieving sub-micron resolutions. Fig. 2 illustrates a comparison of the technologies in terms of their resolution and printing speed. By applying the self-defined nano criterion of $\leq$ 500 nm, several technologies are

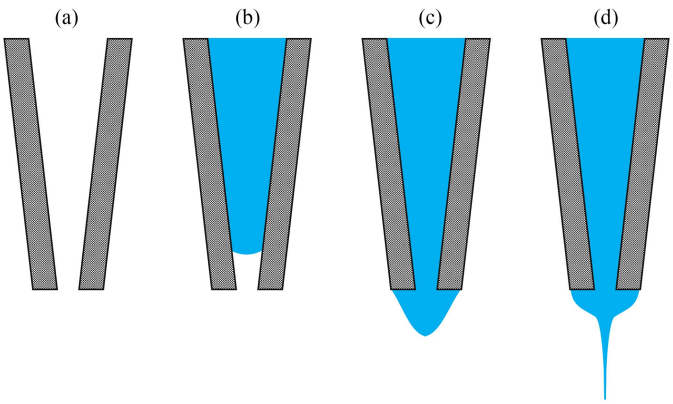

FIGURE 3. Simplified illustration of the electrohydrodynamic printing process, cross-sectional view of one nozzle (a) Empty (b) Back pressure applied (c) Taylor-cone in equilibrium (d) Cone-jetting.

fulfilling this requirement such as: laser-induced photoreduction (also known as two-photon printing), meniscus-confined electroplating, electroplating of locally dispensed ions in liquid (fluidFM or SICM-configurations), focused electron/ion beam induced deposition (FEBID/FIBID) and electrohydrodynamic (EHD) printing.

A. LASER INDUCED PHOTOREDUCTION

Here the metal salt solution is exposed to a laser source resulting in photochemical reduction at the laser focus spot and consequently printing of 3D structures. The photocuring is typically driven by a combination of two photons (two-photon polymerization - 2PP). The major shortcoming is the limited possibility to print materials which in general do not support non-linear absorption, typically opaque materials. In the case of materials with a high refractive index, the resolution can be compromised and interaction between long-wavelength radiation and coinage metals can result in the excitation of plasmonic modes causing the generation of bubbles and deformations [7]. In the review of Harinarayana et al. [8], the technology of laser-induced photoreduction is discussed in detail with the explanation of the process, its possibilities and various applications. One of the highest resolutions achieved so far was presented by Tan et al. [9]. They have produced 15nm thick fibers from the commercially available photo resin SCR500 using two-photon polymerization. This example is an exception in terms of the achieved resolution, but other groups have already presented the fabrication of structures from organic-inorganic hybrid materials [10], metals [11] with resolutions $\leq$ 500 nm and scaffolds of biomaterial [12]. Additionally, the production of silver nitrate structures combined with a polymer matrix has been demonstrated by Maruo et al. [13].

B. MENISCUS-CONFINED ELECTROPLATING

In meniscus-confined electroplating, the nozzle is filled with a metal salt solution and is connected to a backside pressure regulator (typically a pump) to enable the excitation of the solution. The nozzle (or the metal salt solution) and the printing substrate are connected to an electrical power source (typically a direct current (DC) source). Once the metal salt solution is exited from the nozzle, at the interphase point of substate and solution the electrochemical reduction will occur, resulting in 3D metal printing. Minimal resolutions of 100 nm have been reported by Hu et al. [14]. The major drawback of this technology is that the printing substrate needs to be conductive and that it is limited to conductive materials because of the necessity of current flow for deposition. Therefore, the fabrication of structures from different metals such as copper, silver or platinum has already been presented [15] and theoretically the integration of the printing of different metals in one system is also achievable, but not the multi-material printing (polymers, oxides, silicon, carbon etc.) as demonstrated by the other technologies described in this article.

C. ELECTROPLATING OF LOCALLY DISPENSED IONS IN LIQUID

This approach is quite similar to meniscus-confined electroplating. The add-on is the supportive electrolyte bath which is in this case connected to one end of the power supply (again typically DC), while the second end is connected to the metal salt solution. The same shortcoming as in the case of meniscus-confined electroplating is applicable. Minimal resolutions of 400nm have been reported. So far, only printing of metals (copper, platinum and coper-nickel alloy) has been reported. [15], [16] Multi-material printing in one system is hardly possible and additionally the process integration remains a challenge with this technology because the electrolyte bath has a negative effect on already existing structures.

D. FOCUSED ELECTRON/ION BEAM INDUCED DEPOSITION

In the case of the FEBID/FIBID, the precursor gas interacts with the electron/ion beam, resulting in the dissociation of the precursor and consequently 3D printing. The shortcoming of this technology is that the homogeneity of the gas distribution needs to be ensured, resulting in confined space and limited working volume. Processing of large areas or 3D structured substrates as well as the simultaneous multi-material deposition is hardly possible with this technology. For Cryo-FEBID, all of the above is applicable and additionally, the temperature in the print chamber must be held at -155 °C [17]. Minimal resolutions of 1-10nm and the deposition of a variety of single-metal and bi-metal combinations have been reported [18], [19]. Deposition of C, Si, Si_3N_4, SiO_x, TiO_x [20] as well as superconductors [21]. are also reported. However, the deposition of polymer (polymer-like) materials is hardly possible with this technology.

E. EHD PRINTING

Electrohydrodynamic (EHD) printing is a droplet-based technology developed from conventional inkjet printing. Instead of "pushing" the ink out of a nozzle, an electric field between the ink and substrate plate is generated. This electrical field forces charge carriers inside the ink towards the substrate and when the electrostatic force overcomes the surface tension

of the liquid a Taylor cone is formed and nanodroplets or a cone-jet an order of magnitude smaller compared to the used nozzle diameter is ejected. EHD printing requires neither adapted process conditions (high temperature or vacuum) nor electrolytic baths or specially adapted precursor gases. For this reason, there is a high degree of process compatibility and yet even structures smaller than 100 nm can be fabricated with this technology. [22], [23], [24], [25], [26], [27], [28], [29], [30] Furthermore, the printability of many different materials such as metals, semiconductors, polymers, ceramics, carbon nanotubes and graphene has already been demonstrated. [20] In addition, EHD printing is capable of printing large areas due to the relatively high process speed, as can be seen in Fig. 2. This process speed can be multiplied by the use of parallel glass capillary nozzles [31], [32], which also enables simultaneous multi-material printing [33]. In comparison, electrohydrodynamic printing is one of the most promising technologies for the realization of structures with resolutions <500 nm. For this reason, the following chapter summarizes the technological fundamentals, as well as the publications with the highest already achieved resolutions and special applications for the technology.

III. ELECTROHYDRODYNAMIC PRINTING

A. FUNDAMENTALS

The additive manufacturing of structures with the electrohydrodynamic printing process is based on two different forces. The first consists of mechanical pressure applied to the ink by a pump to ensure that the nozzle (Fig. 3(a)) is filled, which is similar to traditional inkjet printing [34]. This pressure has to be adjusted for optimal high-resolution printability so that the ink is getting pushed to the orifice of the nozzle (Fig. 3(b)). In addition to this mechanical pressure, a voltage is applied between the conductive nozzle and the substrate during EHD printing. Due to the high electrical potential of the nozzle, charges are injected into the ink, resulting in the creation of ions in the liquid, which are forced toward the substrate by the applied electric field. This effect is called the injection phenomenon as also explained in more detail by Paillat et al. [35] and is referred back to the experiments of Michael Faraday [36]. The ions accumulate at the lowest point of the meniscus and exert tensile stress on the ink (Fig. 3(c)). By exceeding a threshold value at which the electrostatic force becomes greater than the surface tension of the ink, a stream of ink called cone-jet (Fig. 3(d)) is pulled from the tip of the meniscus and is accelerated to the substrate.

The first observation of electrohydrodynamic jetting was reported by John Zeleny [37] in 1917, who used a 900 μm glass tube to produce a "thread" resp. cone-jet of around 7 μm with ethyl alcohol by applying several thousand volts. He experimentally observed different kinds of jetting e.g., creating droplets or multi-jets by changing the electrical field. In 1964 Sir Geoffrey I. Taylor [38] published his research about the deformation of a liquid's meniscus into a cone shape by well-balanced gravitational, surface tension, internal pressure

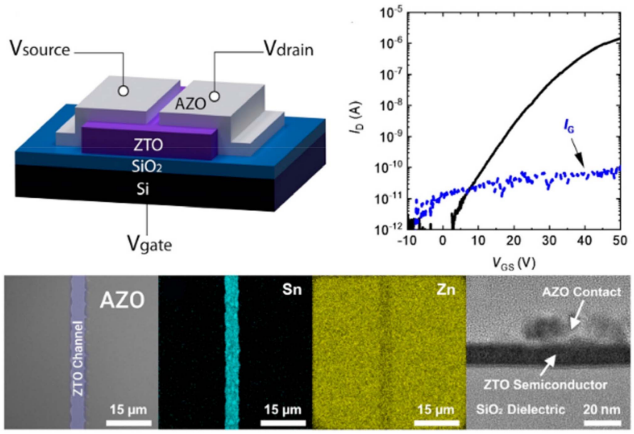

FIGURE 4. Utilization of the EHD-printed PVP line as etch-mask for a photolithography free TFT fabrication. Reproduced with permission. [40] Copyright 2020, American Chemical Society.

and electrostatic forces acting on it. He showed that axial jets can be ejected from the cone of the liquid by increasing the electrical forces and was the first scientist to give a mathematical relationship for the disintegration of liquids under the impact of high electric field strength, which is why the profile, shown in Fig. 3(c), was named after him as Taylor cone.

The first article reporting electrohydrodynamic printing as a separate fabrication technology from electrospinning and electrospraying is published by Park et al. [39] in 2007. It is also the first publication to demonstrate the fabrication of structures in the sub-micrometer range. They used the EHD dripping mode to print 250 nm polyurethane dots on silicon with a 300 nm-internal-diameter nozzle and demonstrated the printing of polymer lines down to 700 nm as etching masks for transistor contacts as an alternative fabrication possibility to the photolithographic process. They also reported the printing of different materials like PEDOT:PSS, silicon-nanoparticles and single-walled carbon nanotubes, but with critical dimensions above one micrometer since the ink properties of these materials are only adjustable to a limited extent.

B. HIGH-RESOLUTION EHD PRINTING

In the last decade, electrohydrodynamic printing of critical dimensions in the nanometer range with many different materials has been published. Most publications describe the printing of organic materials because their properties are easier to tailor to the requirements of electrohydrodynamic printing. Cho et al. [40] printed 312 nm PVP-polymer lines with a 1 μm capillary nozzle on silicon. As an alternative method, they demonstrated subtractive printing of PMMA by jetting the solvent and produced masks for non-printable materials. They used this technique to fabricate a bottom-gate, top-contact thin film transistor without any photolithographic processing. The design of the transistor as well as its output characteristics are shown in Fig. 4. Another application for nano/micro-manufacturing of polymers is the fabrication of cellular structures for tissue engineering as shown by Zhang et al. [41] They used EHD-cone-jetting of PEO-PCL

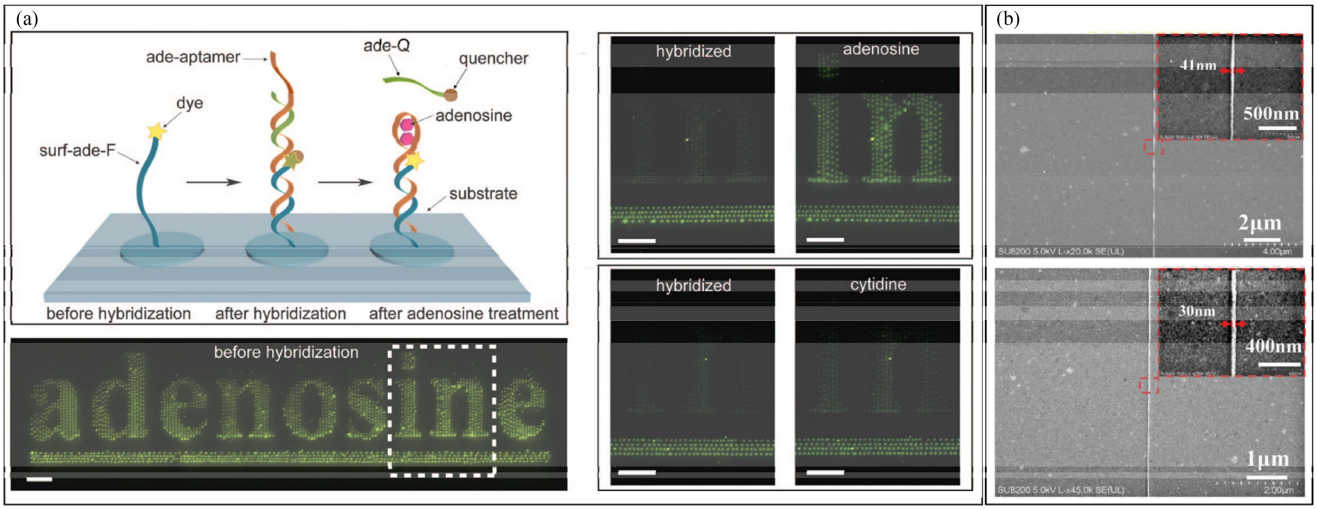

FIGURE 5. **(a) EHD-printing of DNA droplets for biosensing applications. Reproduced with permission [42] Copyright 2008, American Chemical Society (b) High-resolution PEO lines fabricated by microtip focused EHD-printing. Reproduced with permission [29] Copyright 2009, Royal Society of Chemistry.**

biopolymer lines on silicon down to 130 nm line width to build the scaffold for improved cell adhesion. In combination with the possibility of stacking several printing layers on top of each other, the production of the scaffold by EHD printing is a promising method for enhanced tissue regeneration. The deposition of DNA droplets with a minimum size of 100 nm has also already been demonstrated with electrohydrodynamic printing by Park et al. [42] as illustrated in Fig. 5(a). They proposed that this technique can be applied to the alignment of DNA nanoparticles and the biosensing of RNA constituents.

Even the production of structures below 100nm has already been presented with the technology of electrohydrodynamic printing. Zou et al. [27] reported cone-jetting of 68 nm photoresist lines on gold with a 2 μm-inner-diameter capillary. Their work demonstrated the capability to use EHD printing as an alternative approach for the rapid additive manufacturing of etch masks. Another approach to fabricate masks for etching by EHD-printing is shown by Su et al. [29]. They conducted a study on the dependence of the electrical signal characteristics such as bias voltage, pulse amplitude, duty cycle and pulse frequency on the droplet diameter. With their optimized process parameters, they demonstrated cone-jetting of 90 nm NOA-61 UV-curable adhesive droplets and PEO lines widths down to 30 nm as shown in Fig. 5(b). Furthermore, self-aligning materials such as PS-b-PMMA block-copolymers are promising materials to reduce the resolution of printed structures even further as reported by Onses et al. [28]. They used a 1μm capillary nozzle to print lines with 800 nm width, but thermal annealing results in the self-assembly of the polymer to even smaller structures of around 50 nm.]

C. UNIQUE APPLICATIONS OF EHD PRINTING

The technology of electrohydrodynamic printing can also be utilized for diverse applications. Kim et al. [43] demonstrated cone-jetting of semiconductor particles dissolved in dichlorobenzene. They printed lines down to 410 nm for the potential fabrication of micro-LEDs on a glass substrate. Another different approach to traditional EHD printing is reported by Wang et al. [30]. They reported cone-jetting 40nm PZT nanowires by using an outer high viscous silicone solution to stabilize the inner functional ink. After completing the printing, the abundant silicone had to be removed. That is the reason why this process is only semi-additive and can't be scaled to high throughput, but it is a possible way to fabricate PZT structures for nanoscale piezoelectric applications. In addition, the printing of metallic structures by nanoparticle suspensions has been demonstrated. Lee et al. [44] presented the EHD-printing of a silver nanowire tip (height: ~4.5 μm, body diameter: ~150 nm) on an AFM-cantilever for deep trench profile measurements as illustrated in Fig. 6(a). They reported the simplicity and flexibility of fabricating different measurement tip sizes by adjusting the substrate-nozzle-distance printing process parameters. Furthermore, Schneider et al. [25] and Rohner et al. [45] reported the nanoscale fabrication of conductive nanoparticle materials by printing silver and gold grids and walls with a line width down to 80 nm as illustrated in Fig. 6(b). By applying an AC voltage charge agglomeration on the borosilicate substrates can be prevented to fabricate conductive and transparent grids exceeding the optoelectronic performance of conventional ITO. Rohner et al. investigated the electrical properties of the gold nanoparticles and showed that the resistivity of the printed nanowalls was only 2.5 times that of bulk gold. Additionally, Schneider et al. [24] demonstrated the printing of 50 nm thick 3D-gold scaffolds on cyclic olefin copolymer with a potential biomedical application in monitoring cancer cell migration. Galliker et al. [23] reported the fabrication of 60 nm gold lines and 75 nm diameter gold nanopillars. These pillars are adjustable in their angle and show great potential for the development of nanoantennas. Reiser et al. [22] presented an even more advanced approach for EHD printing by generating metal ions directly within the nozzles via the electro-corrosion of a metal

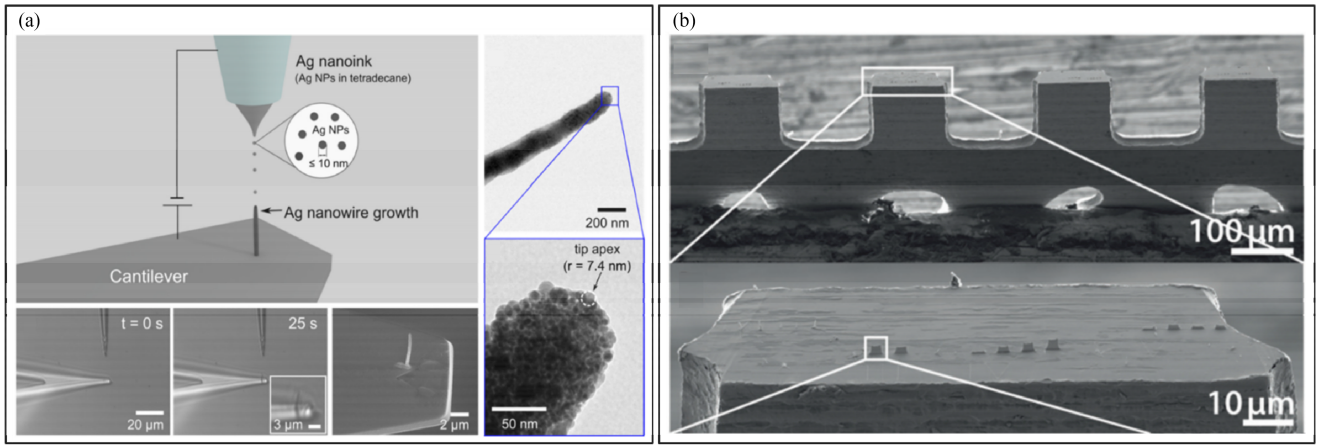

FIGURE 6. **(a) EHD-printing of silver nanoparticle pillars on cantilevers for AFM-measurements. Reproduced with permission [44] Copyright 2020, American Chemical Society (b) Fabrication of 100nm wide gold walls with 2.5 times resistivity of bulk gold. Reproduced with permission [45] Copyright 2020, the Royal Society of Chemistry.**

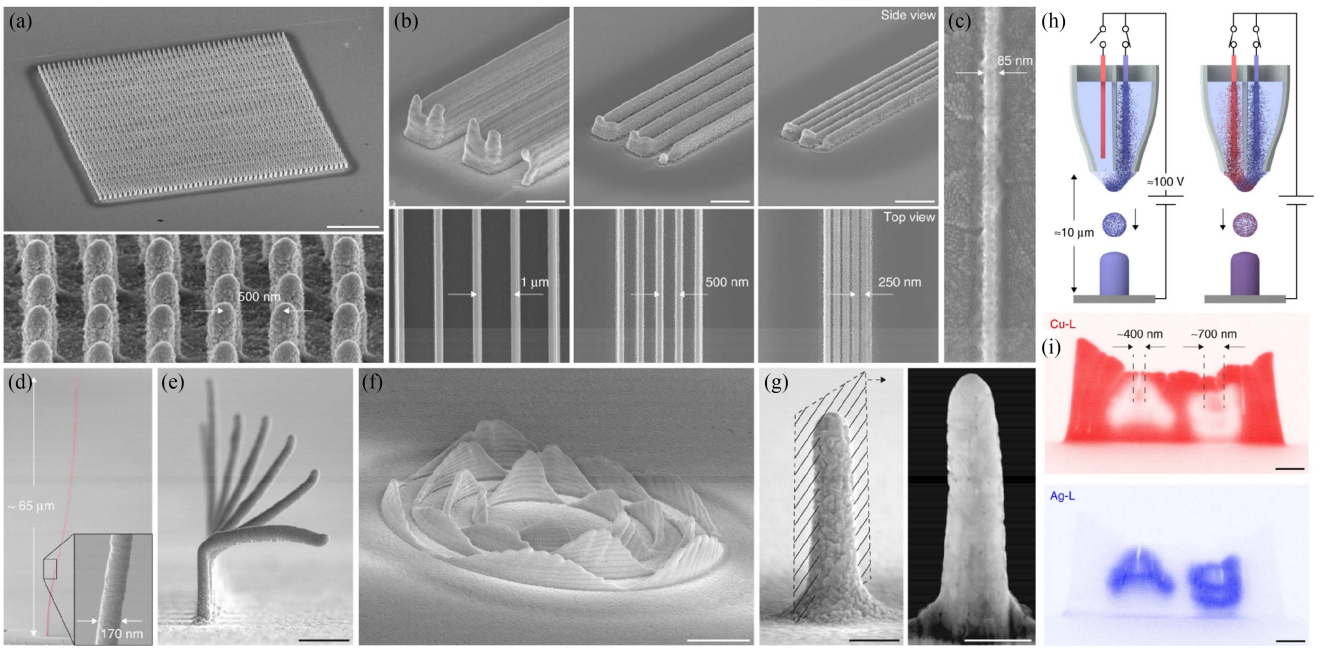

FIGURE 7. **Multimaterial redox printing as advanced EHD printing technique. Reproduced with permission [22] Copyright 2019, the Author(s) (a) Array of Cu pillars printed with a point-to-point spacing of 500 nm. Scale bar: 5 μm (b) Walls printed at decreasing wall-to-wall spacing. scale bars: 1 μm (c) Printed Cu line (d) Cu wire with an aspect ratio of approximately 400 (e) Overhangs formed by a lateral translation of the stage balancing the out-of-plane growth rate. scale bar: 1 μm (f) Concentric, out-of-plane sine waves printed with a layer-by-layer strategy.scale bar: 2 μm (g) as-printed Cu pillar and corresponding cross-section showing the dense, polycrystalline microstructure. scale bars: 200 nm (h) Schematic of the multimaterial redox printing (i) Cu-L and Ag-L EDX element map of a heterogeneous structure printed using a single nozzle. scale bars: 1 μm.**

electrode. They demonstrated multi-material printing through the combination of a silver and copper electrode in separate chambers of one nozzle. Switches controlled the flow of electric charge, changing which metal was printed. Absorption of positive charge in the electrode produces positive metal ions in the solution. Due to this, it is possible to print those two materials simultaneously or alternating depending on the applied voltage signal. They presented various 3D structures e.g., pillars, walls or microwires with the smallest line width of 85nm as illustrated in Fig. 7.

IV. SUMMARY

This article summarizes the additive manufacturing technologies capable of fabricating structures $\leq$ 500 nm and briefly describes their process-related characteristics. The following section describes the EHD printing process and presents the possibilities of this technology. It is shown that a wide range of organic and inorganic materials can be processed and that by optimizing the parameters and the ink, structures with resolutions even below 100 nm can be manufactured. Due to the unique properties of the technology, even simple 3D

structures such as free-standing pillars or nanowalls can be fabricated without intermediate treatments (curing/drying).

However, EHD printing is also facing limitations that prevent the technology from being utilized for industrial applications. On the one hand, all the systems presented are equipped with only a single nozzle, which means that throughput is very slow. The use of glass capillary nozzles prevents the technology from reaching industrial scalability since the electric fields of several glass nozzles would mutually interfere with each other and hence negatively affect the printing process. In addition, the electric field is generated between the top of the process table and the ink. The use of non-planar substrates or substrates composed of different materials also leads to a change in the electric field, which ultimately affects the generation of droplets or the cone jet and causes process instabilities.

Nevertheless, electrohydrodynamic printing has decisive advantages compared to other technologies for the additive manufacturing of sub-micrometer structures. For EHD printing no electrolytic baths or a special pre-treatment of substrates are necessary, which enables a high variability of processable substrates e.g., also with biodegradable and biocompatible properties and allows straightforward integration into microfabrication process lines. Furthermore, no prefabricated carrier substrates or precisely controlled process environments (vacuum chambers, process gases, high temperatures, etc.) are required. These aspects distinguish the EHD method from the other processes reviewed by Hirt et al. [3], which is why electrohydrodynamic printing is currently one of the most promising technologies for the additive manufacturing of features in the nanometer range.

REFERENCES

[1] M. C. Fuentes, *The Electronic Components & Systems (ECS) Strategic Research and Innovation Agenda (SRIA)*. Berlin, Germany: ECS, 2021. [Online]. Available: https://ecscollaborationtool.eu/publication/download/2021-01-11-ecs-sria2021-final.pdf

[2] C. Liu et al., "3D printing technologies for flexible tactile sensors toward wearable electronics and electronic skin," *Polymers*, vol. 10, no. 6, pp. 1–31, 2018, doi: 10.3390/polym10060629.

[3] L. Hirt, A. Reiser, R. Spolenak, and T. Zambelli, "Additive manufacturing of metal structures at the micrometer scale," *Adv. Mater.*, vol. 29, no. 17, 2017, Art. no. 1604211, doi: 10.1002/adma.201604211.

[4] A. Reiser et al., "Metals by micro-scale additive manufacturing: Comparison of microstructure and mechanical properties," *Adv. Funct. Mater.*, vol. 30, no. 28, Art. no. 1910491, 2020, doi: 10.1002/adfm.201910491.

[5] M. Criado-Gonzalez, A. Dominguez-Alfaro, N. Lopez-Larrea, N. Alegret, and D. Mecerreyes, "Additive manufacturing of conducting polymers: Recent advances, challenges, and opportunities," *ACS Appl. Polym. Mater.*, vol. 3, no. 6, pp. 2865–2883, 2021, doi: 10.1021/acsapm.1c00252.

[6] H. Abdolmaleki, P. Kidmose, and S. Agarwala, "Droplet-based techniques for printing of functional inks for flexible physical sensors," *Adv. Mater.*, vol. 33, no. 20, pp. 1–29, 2021, doi: 10.1002/adma.202006792.

[7] M. Carlotti and V. Mattoli, "Functional materials for two-photon polymerization in microfabrication," *Small*, vol. 15, no. 40, Oct. 2019, Art. no. 1902687, doi: 10.1002/smll.201902687.

[8] V. Harinarayana and Y. C. Shin, "Two-photon lithography for three-dimensional fabrication in micro/nanoscale regime: A comprehensive review," *Opt. Laser Technol.*, vol. 142, Oct. 2021, Art. no. 107180, doi: 10.1016/j.optlastec.2021.107180.

[9] D. Tan et al., "Reduction in feature size of two-photon polymerization using SCR500," *Appl. Phys. Lett.*, vol. 90, no. 7, Feb. 2007, Art. no. 071106, doi: 10.1063/1.2535504.

[10] E. Kabouraki, A. N. Giakoumaki, P. Danilevicius, D. Gray, M. Vamvakaki, and M. Farsari, "Redox multiphoton polymerization for 3D nanofabrication," *Nano Lett.*, vol. 13, no. 8, pp. 3831–3835, Aug. 2013, doi: 10.1021/nl401853k.

[11] Y.-Y. Cao, N. Takeyasu, T. Tanaka, X.-M. Duan, and S. Kawata, "3D metallic nanostructure fabrication by surfactant-assisted multiphoton-induced reduction," *Small*, vol. 5, no. 10, pp. 1144–1148, Mar. 2009, doi: 10.1002/smll.200801179.

[12] A. Ovsianikov, V. Mironov, J. Stampfl, and R. Liska, "Engineering 3D cell-culture matrices: Multiphoton processing technologies for biological and tissue engineering applications," *Expert Rev. Med. Devices*, vol. 9, no. 6, pp. 613–633, Nov. 2012, doi: 10.1586/erd.12.48.

[13] S. Maruo and T. Saeki, "Femtosecond laser direct writing of metallic microstructures by photoreduction of silver nitrate in a polymer matrix," *Opt. Exp.*, vol. 16, no. 2, pp. 1174–1179, 2008, doi: 10.1364/OE.16.001174.

[14] J. Hu and M.-F. Yu, "Meniscus-confined three-dimensional electrodeposition for direct writing of wire bonds," *Science*, vol. 329, no. 5989, pp. 313–316, Jul. 2010, doi: 10.1126/science.1190496.

[15] L. Hirt et al., "Template-free 3D microprinting of metals using a force-controlled nanopipette for layer-by-layer electrodeposition," *Adv. Mater.*, vol. 28, no. 12, pp. 2311–2315, Mar. 2016, doi: 10.1002/adma.201504967.

[16] J. D. Whitaker, J. B. Nelson, and D. T. Schwartz, "Electrochemical printing: Software reconfigurable electrochemical microfabrication," *J. Micromechanics Microengineering*, vol. 15, no. 8, pp. 1498–1503, Aug. 2005, doi: 10.1088/0960-1317/15/8/017.

[17] M. Bresin, M. Toth, and K. A. Dunn, "Direct-write 3D nanolithography at cryogenic temperatures," *Nanotechnology*, vol. 24, no. 3, Dec. 2012, Art. no. 035301, doi: 10.1088/0957-4484/24/3/035301.

[18] C. W. Hagen, "The future of focused electron beam-induced processing," *Appl. Phys. A*, vol. 117, no. 4, pp. 1599–1605, Nov. 2014, doi: 10.1007/S00339-014-8847-8.

[19] A. Botman, J. J. L. Mulders, and C. W. Hagen, "Creating pure nanostructures from electron-beam-induced deposition using purification techniques: A technology perspective," *Nanotechnology*, vol. 20, no. 37, Sep. 2009, Art. no. 372001, doi: 10.1088/0957-4484/20/37/372001.

[20] M. S. Onses, E. Sutanto, P. M. Ferreira, A. G. Alleyne, and J. A. Rogers, "Mechanisms, capabilities, and applications of high-resolution electrohydrodynamic jet printing," *Small*, vol. 11, no. 34, pp. 4237–4266, Sep. 2015, doi: 10.1002/smll.201500593.

[21] J. L. Arias et al., "Superconducting materials and devices grown by focused ion and electron beam induced deposition," *Nanomaterials*, vol. 12, no. 8, Apr. 2022, Art. no. 1367, doi: 10.3390/NANO12081367.

[22] A. Reiser et al., "Multi-metal electrohydrodynamic redox 3D printing at the submicron scale," *Nature Commun.*, vol. 10, no. 1, pp. 1–8, 2019, doi: 10.1038/s41467-019-09827-1.

[23] P. Galliker, J. Schneider, H. Eghlidi, S. Kress, V. Sandoghdar, and D. Poulikakos, "Direct printing of nanostructures by electrostatic autofocussing of ink nanodroplets," *Nature Commun.*, vol. 3, pp. 890–899, May 2012, doi: 10.1038/ncomms1891.

[24] J. Schneider et al., "A novel 3D integrated platform for the high-resolution study of cell migration plasticity," *Macromol. Biosci.*, vol. 13, no. 8, pp. 973–983, 2013, doi: 10.1002/mabi.201200416.

[25] J. Schneider, P. Rohner, D. Thureja, M. Schmid, P. Galliker, and D. Poulikakos, "Electrohydrodynamic nanodrip printing of high aspect ratio metal grid transparent electrodes," *Adv. Funct. Mater.*, vol. 26, no. 6, pp. 833–840, 2016, doi: 10.1002/adfm.201503705.

[26] P. Galliker, J. Schneider, and D. Poulikakos, "Dielectrophoretic bending of directly printed free-standing ultra-soft nanowires," *Appl. Phys. Lett.*, vol. 104, no. 7, Feb. 2014, Art. no. 073105, doi: 10.1063/1.4866002.

[27] W. Zou, H. Yu, P. Zhou, Y. Zhong, Y. Wang, and L. Liu, "High-resolution additive direct writing of metal micro/nanostructures by electrohydrodynamic jet printing," *Appl. Surf. Sci.*, vol. 543, Dec. 2021, Art. no. 148800, doi: 10.1016/j.apsusc.2020.148800.

[28] M. S. Onses et al., "Hierarchical patterns of three-dimensional block-copolymer films formed by electrohydrodynamic jet printing and self-assembly," *Nature Nanotechnol.*, vol. 8, no. 9, pp. 667–675, 2013, doi: 10.1038/nnano.2013.160.

[29] S. Su, J. Liang, Z. Wang, W. Xin, X. Li, and D. Wang, "Microtip focused electrohydrodynamic jet printing with nanoscale resolution," *Nanoscale*, vol. 12, no. 48, pp. 24450–24462, 2020, doi: 10.1039/d0nr08236h.

[30] D. Wang et al., "Nanoscale coaxial focused electrohydrodynamic jet printing," *Nanoscale*, vol. 10, no. 21, pp. 9867–9879, 2018, doi: 10.1039/c8nr01001c.

[31] Y. Pan, Y. A. Huang, L. Guo, Y. Ding, and Z. Yin, "Addressable multi-nozzle electrohydrodynamic jet printing with high consistency by multi-level voltage method," *AIP Adv.*, vol. 5, no. 4, 2015, Art. no. 047108, doi: 10.1063/1.4917300.

[32] A. Khan, K. Rahman, M. T. Hyun, D. S. Kim, and K. H. Choi, "Multi-nozzle electrohydrodynamic inkjet printing of silver colloidal solution for the fabrication of electrically functional microstructures," *Appl. Phys. A Mater. Sci. Process.*, vol. 104, no. 4, pp. 1113–1120, 2011, doi: 10.1007/s00339-011-6386-0.

[33] M. Chen et al., "Parallel, multi-material electrohydrodynamic 3D nanoprinting," *Small*, vol. 16, no. 13, 2020, Art. no. 1906402, doi: 10.1002/smll.201906402.

[34] K. Barton, S. Mishra, K. A. Shorter, A. Alleyne, P. Ferreira, and J. Rogers, "A desktop electrohydrodynamic jet printing system," *Mechatronics*, vol. 20, no. 5, pp. 611–616, Aug. 2010, doi: 10.1016/j.mechatronics.2010.05.004.

[35] T. Paillat and G. Touchard, "Electrical charges and liquids motion," *J. Electrostatics*, vol. 67, no. 2/3, pp. 326–334, 2009, doi: 10.1016/j.elstat.2009.01.038.

[36] M. V. Faraday, "Experimental researches in electricity," *Philos. Trans. Roy. Soc. London*, vol. 122, pp. 125–162, Dec. 1832, doi: 10.1098/rstl.1832.0006.

[37] J. Zeleny, "Instability of electrified liquid surfaces," *Phys. Rev.*, vol. 10, no. 1, pp. 1–6, Jul. 1917, doi: 10.1103/PhysRev.10.1.

[38] G. I. S. Taylor, "Disintegration of water drops in an electric field," *Proc. Roy. Soc. London Ser. A Math. Phys. Sci.*, vol. 280, no. 1382, pp. 383–397, Jul. 1964, doi: 10.1098/rspa.1964.0151.

[39] J. U. Park et al., "High-resolution electrohydrodynamic jet printing," *Nature Mater.*, vol. 6, no. 10, pp. 782–789, 2007, doi: 10.1038/nmat1974.

[40] T. H. Cho et al., "Area-selective atomic layer deposition patterned by electrohydrodynamic jet printing for additive manufacturing of functional materials and devices," *ACS Nano*, vol. 14, no. 12, pp. 17262–17272, 2020, doi: 10.1021/acsnano.0c07297.

[41] B. Zhang, J. He, Q. Lei, and D. Li, "Electrohydrodynamic printing of sub-microscale fibrous architectures with improved cell adhesion capacity," *Virtual Phys. Prototyping*, vol. 15, no. 1, pp. 62–74, 2020, doi: 10.1080/17452759.2019.1662991.

[42] J.-U. Park, J. H. Lee, U. Paik, Y. Lu, and J. A. Rogers, "Nanoscale patterns of oligonucleotides formed by electrohydrodynamic jet printing with applications in biosensing and nanomaterials assembly," *Nano Lett.*, vol. 8, no. 12, pp. 4210–4216, Dec. 2008, doi: 10.1021/nl801832v.

[43] B. H. Kim et al., "High-resolution patterns of quantum dots formed by electrohydrodynamic jet printing for light-emitting diodes," *Nano Lett.*, vol. 15, no. 2, pp. 969–973, 2015, doi: 10.1021/nl503779e.

[44] H. Lee et al., "On-demand 3D printing of nanowire probes for high-aspect-ratio atomic force microscopy imaging," *ACS Appl. Mater. Interfaces*, vol. 12, no. 41, pp. 46571–46577, 2020, doi: 10.1021/acsami.0c14148.

[45] P. Rohner et al., "3D electrohydrodynamic printing and characterisation of highly conductive gold nanowalls," *Nanoscale*, vol. 12, no. 39, pp. 20158–20164, 2020, doi: 10.1039/d0nr04593d.